

Molecular and Cellular Biology

Specific Isoforms of Translation Initiation Factor 4GI Show Differences in Translational Activity

Mark J. Coldwell and Simon J. Morley

Mol. Cell. Biol. 2006, 26(22):8448. DOI:

10.1128/MCB.01248-06.

Published Ahead of Print 18 September 2006.

Updated information and services can be found at:
<http://mcb.asm.org/content/26/22/8448>

SUPPLEMENTAL MATERIAL

These include:

[Supplemental material](#)

REFERENCES

This article cites 50 articles, 34 of which can be accessed free at: <http://mcb.asm.org/content/26/22/8448#ref-list-1>

CONTENT ALERTS

Receive: RSS Feeds, eTOCs, free email alerts (when new articles cite this article), [more»](#)

Information about commercial reprint orders: <http://journals.asm.org/site/misc/reprints.xhtml>
To subscribe to to another ASM Journal go to: <http://journals.asm.org/site/subscriptions/>

Journals.ASM.org

Specific Isoforms of Translation Initiation Factor 4GI Show Differences in Translational Activity^{∇†}

Mark J. Coldwell and Simon J. Morley*

Department of Biochemistry, School of Life Sciences, University of Sussex, Falmer, Brighton BN1 9QG, United Kingdom

Received 10 July 2006/Returned for modification 1 August 2006/Accepted 1 September 2006

The eukaryotic initiation factor (eIF) 4GI gene locus (eIF4GI) contains three identified promoters, generating alternately spliced mRNAs, yielding a total of five eIF4GI protein isoforms. Although eIF4GI plays a critical role in mRNA recruitment to the ribosomes, little is known about the functions of the different isoforms, their partner binding capacities, or the role of the homolog, eIF4GII, in translation initiation. To directly address this, we have used short interfering RNAs (siRNAs) expressed from DNA vectors to silence the expression of eIF4GI in HeLa cells. Here we show that reduced levels of specific mRNA and eIF4GI isoforms in HeLa cells promoted aberrant morphology and a partial inhibition of translation. The latter reflected dephosphorylation of 4E-BP1 and decreased eIF4F complex levels, with no change in eIF2 α phosphorylation. Expression of siRNA-resistant Myc-tagged eIF4GI isoforms has allowed us to show that the different isoforms exhibit significant differences in their ability to restore translation rates. Here we quantify the efficiency of eIF4GI promoter usage in mammalian cells and demonstrate that even though the longest isoform of eIF4GI (eIF4Glf) was relatively poorly expressed when reintroduced, it was more efficient at promoting the translation of cellular mRNAs than the more highly expressed shorter isoforms used in previous functional studies.

Translational control plays a critical role in overall gene expression, allowing the rapid and reversible stimulation of protein synthesis from preexisting mRNAs, the fine-tuning of protein expression levels, and in some cases the production of proteins at specific sites in the cell (reviewed in reference 37). Eukaryotic protein synthesis comprises three stages: initiation, elongation, and termination. The initiation phase refers to the binding of the ribosomal subunits to the mRNA and positioning of the subunits at the first codon of the mRNA open reading frame. Several eukaryotic initiation factors (eIFs) are required for this process, and in most cases, initiation determines both the rate of translation of individual mRNAs and the overall rate of protein synthesis (17, 19, 32, 36). The inappropriate expression of several initiation factors has been noted for a number of diseases and cancers (1, 34), and the improper recruitment of mRNAs to the ribosome may also play a role in the deregulation of gene expression.

The multidomain factor eIF4G, expressed as two isoforms in mammalian cells sharing 46% identity at the amino acid level (eIF4GI/II), plays an essential role in mRNA recruitment by acting as a molecular focal point upon which the translation initiation complex is assembled to bring together the mRNA and the ribosome. eIF4G is part of the eIF4F complex (17, 36), which also comprises the mRNA cap-binding protein (eIF4E) and an ATP-dependent RNA helicase activity (eIF4A, in concert with eIF4B). The yeast, wheat, and mammalian homologs bind to RNA in a sequence-independent manner (6, 28, 30), although mammalian eIF4G also binds specifically to the 5'

untranscribed region of the encephalomyocarditis virus RNA genome, which contains an internal ribosome entry segment (IRES) (30, 41). Interaction of the poly(A) binding protein (PABP) with the N terminus of eIF4G (23), the kinase that phosphorylates eIF4E (Mnk1) with the C terminus of eIF4G (45) and the multisubunit eIF3 (and therefore the 40S ribosomal subunit and eIF2-GTP-initiator methionyl tRNA complex) with the central portion of eIF4G, completes the formation of the 48S preinitiation complex (17, 37).

Consistent with an important regulatory role, the expression level of eIF4G is low in both mammalian and yeast cells, and its down-regulation by proteolysis is an early response to the induction of apoptosis or infection by some viruses (reviewed in reference 37). The importance of regulating the level of expression of eIF4G is demonstrated by the finding that amplification of overall eIF4GI protein levels occurs in squamous cell lung carcinoma (3) and breast carcinoma (2), while overexpression of cDNA encoding the shortest isoform of eIF4GI causes the malignant transformation of mammalian cell lines (14, 22). The original cDNA clone of eIF4GI (52) was extended in a later study (23) to identify the PABP binding site. The independent discovery of a further N-terminal extension of 40 amino acids finally identified the longest possible open reading frame of eIF4GI (7, 9), with these studies suggesting alternative translation initiation can generate five isoforms of eIF4GI. The identification of three promoters within the eIF4GI gene locus and the finding that mRNAs from one of these promoters are also alternately spliced (10) indicate that there are multiple levels at which the expression of eIF4GI can be regulated. Until recently, no evidence had been found for differential activities between eIF4GI and eIF4GII, since the two proteins could functionally complement each other in various translation assays. However, an important difference has recently been revealed with the discovery that during megakaryocytic differentiation, eIF4GII is selectively recruited into eIF4F

* Corresponding author. Mailing address: Department of Biochemistry, School of Life Sciences, University of Sussex, Falmer, Brighton BN1 9QG, United Kingdom. Phone: 44 (0) 1273 678544. Fax: 44 (0) 1273 678433. E-mail: s.j.morley@sussex.ac.uk.

† Supplemental material for this article may be found at <http://mcb.asm.org/>.

[∇] Published ahead of print on 18 September 2006.

complexes (11). In addition, eIF4G homologues differ in their phosphorylation status, with serum-stimulated sites of phosphorylation identified in the C terminus of eIF4GI but not in eIF4GII (44, 46), suggesting a possible isoform-specific role for this modification. In contrast, eIF4GII phosphorylation is increased primarily at the G₂/M phase of the cell cycle (44, 46), when there is a transient decrease in overall translation rates, although it remains unclear how these individual phosphorylation events modulate translation.

Since eIF4G plays such a central role in the assembly of the preinitiation complex, it is not surprising that modifications of eIF4GI and eIF4GII by physiological cleavage events have drastic consequences for translation initiation (reviewed in references 37 and 43). Cleavage of eIF4GI and eIF4GII by picornavirus proteases (leader or 2A protease) leads to the separation of the region involved in mRNA cap binding from the ribosome binding portion of the molecule (reviewed in reference 38). This results in a severe, selective inhibition of host protein synthesis, with the C-terminal fragment of eIF4G functioning in a modified preinitiation complex to allow translation of uncapped viral RNA and certain cellular IRES-containing mRNAs (5, 25). Human immunodeficiency virus type 1 protease-mediated cleavage of eIF4GI but not eIF4GII has also been observed (40, 51), with both eIF4GI and eIF4GII being targets for caspase-mediated degradation during apoptosis (37).

However, in spite of this knowledge, little is currently known about the partner binding capacities or function of the different isoforms and variants of eIF4G in translation initiation. To directly address the role for the different full-length isoforms of eIF4GI in vivo, we have used short interfering RNAs (siRNAs) expressed from DNA vectors (49) to reduce the expression of eIF4GI in HeLa cells (21), causing morphological changes and a partial inhibition of translation rates. The latter could be ascribed to a general dephosphorylation of 4E-BP1 and decreased eIF4F complex levels, with no change in eIF2 α phosphorylation. Upon expression, the siRNA-resistant Myc-tagged eIF4GI isoforms were able to form eIF4F complexes in line with the binding sites present in the molecules. However, even though the eIF4GI α isoform was relatively poorly expressed, it was significantly more efficient at promoting translation than the highly expressed, shortest isoform of eIF4GI used in previous studies.

MATERIALS AND METHODS

Plasmids expressing siRNA hairpins and eIF4G sequences. Details of oligonucleotide primers used are provided in the supplemental material. In all cases, the presence of the correct siRNA or eIF4G sequence was verified by restriction digestion and automated sequencing. A reference plasmid for the quantitative real-time PCR assays containing a single copy of each amplicon was created by deleting a 3.7-kb BglII-to-SpeI fragment from pSPORT4GI (a kind gift from Richard Lloyd) to make p Δ 4GI. Two cDNAs corresponding to the α and γ amplicons were amplified from cDNA made from total HeLa RNA with the Improm II reverse transcription system (Promega) using random primers. The α amplicon, amplified with primers RT α F and RT α R, and the γ amplicon, amplified with primers RT γ F and RT γ R, were inserted into the BspEI and XbaI sites of p Δ 4GI, respectively. Three potential siRNA target sites (si2, si5, and si31) were identified in the N terminus of the eIF4GI sequence using the siRNA design tool (www.ambion.com), and corresponding oligonucleotides were inserted into the pSilencer 3.0 H1 plasmid (Ambion). A control siRNA that corresponded to each eIF4GI-specific siRNA was created that contained mismatches to the center of the target site and oligonucleotides inserted into the same vector. A plasmid to quantify the effects of siRNA-mediated silencing of eIF4GI mRNA was created by amplifying a fragment of

the plasmid pcDNAmN-FAGf (12) with primers siCH F and 4G-N R and inserting the XhoI-digested product into the vector psiCHECK2 digested with the same enzyme (Promega). *Renilla* and firefly luciferase activities were measured using the dual-luciferase reporter assay system as per the manufacturer's instructions (Promega). The vector pcDNAmyc and variants containing the five different eIF4GI open reading frames or the middle apoptotic cleavage fragment M-FAG have been previously described (12). The QuikChange site-directed mutagenesis method (Stratagene) and the primers si31mutF and si31mutR were used to introduce three nucleotide changes in vectors containing eIF4GI cDNA sequences that would maintain the correct protein sequence but prevent siRNA-mediated degradation of the exogenous mRNA. In addition, we subcloned the eIF4GII open reading frame encoding the previously published sequence (18) by reverse transcription (RT)-PCR from HeLa cell mRNA using the StrataScript One-Tube RT-PCR kit with the Easy-A PCR cloning enzyme (Stratagene) and the primers 4GII5'F, 4GII5'R, 4GII3'F, and 4GII3'R. Following amplification, the resultant eIF4GII 5' and 3' cDNAs were ligated into pGEM T-Easy (Promega). The cDNAs were introduced into the pcDNAmyc vector in two steps. First, the 5' eIF4GII cDNA was inserted between the HindIII and NotI sites of pcDNAmyc. This vector was digested with BspEI and NotI, and the 3' eIF4GII cDNA was inserted via the same sites.

Cell culture and transient transfection. Materials for tissue culture were from Invitrogen (United Kingdom), and fetal calf serum was from Labtech International (United Kingdom). HeLa, HEK293, and MCF7 cells were obtained from the European Collection of Cell Cultures and maintained in Dulbecco's modified Eagle's medium (HeLa and HEK293) or RPMI (MCF7) supplemented with 10% fetal bovine serum at 37°C in a humidified atmosphere containing 5% CO₂. Cells were seeded on 5-cm plates at a density of 100,000 cells per plate. Twenty-four hours later, 1 μ g of pSilencer DNA and 2 μ g of isoform-specific pcDNAm4G or 1 μ g of pcDNAmM-FAG was transfected into each well using FuGene 6 (Roche, United Kingdom), according to the manufacturer's protocols. The transfection mixture was removed 24 h later, and the cells were washed twice with phosphate-buffered saline (PBS) before being incubated for a further 48 or 72 h in fresh media.

Northern blotting and quantitative RT-PCR. Total cellular RNA was isolated using the RNeasy kit (Ambion) according to the manufacturer's protocol. Equal amounts of RNA were subjected to denaturing agarose gel electrophoresis using the NorthernMax kit (Ambion). Prior to Northern blotting, RNA was visualized with Radiant Red staining (Bio-Rad) and then transferred from the gel to a Zetaprobe nitrocellulose membrane (Bio-Rad) using capillary blotting. A random-primed, radiolabeled probe against eIF4GI was created by digesting pcDNAmC-FAG (12) with HindIII and XhoI. The 1.3-kb fragment encoding C-FAG was isolated and labeled with [α -³²P]dCTP (800 Ci/mmol) using the RadPrime DNA labeling system (Invitrogen). Unincorporated nucleotides were removed by passing the probe through a NucAway column (Ambion). The probe was hybridized to the membrane overnight and, following washing, was detected by phosphorimager analysis. A control probe against β -actin was then hybridized to the membrane and visualized in the same way. Total cDNA for the quantitative PCR assay was prepared from total RNA with the Improm II reverse transcription system (Promega) using random primers. The QuantiTect SYBR Green PCR kit (QIAGEN) was used to detect different species of eIF4GI mRNA or glyceraldehyde-3-phosphate dehydrogenase (GAPDH) mRNA, using the primers described in the supplemental material, which were designed using Primer Express Program v2.0 (Applied Biosystems). Amplification reactions were carried out and analyzed using an Applied Biosystems 7500 real-time PCR system.

Preparation of cell lysates and measurement of protein synthesis rates. Cells were harvested by scraping into ice-cold PBS containing 40 mM β -glycerophosphate and 2 mM benzamide. Following centrifugation for 1 min at 10,000 \times g, cells were resuspended in buffer A (20 mM morpholinepropanesulfonic acid-KOH, pH 7.4; 25 mM KCl; 2 mM MgCl₂; 2 mM benzamide; 2 mM Na₃VO₄; 1 μ M microcystin; 2 mM EGTA; 20 mM NaF; 0.1 mM GTP, 10% [vol/vol] glycerol; 1 \times Complete EDTA-free protease inhibitor cocktail [Roche]) and lysed by the addition of 0.5% (vol/vol) Igepal and 0.5% (vol/vol) deoxycholate. Nuclei and insoluble protein were removed by centrifugation for 5 min at 10,000 \times g and 4°C, and the resulting supernatant was snap frozen in liquid N₂. To determine protein synthesis rates after 96 h of transfection, the conditioned medium was supplemented with 33 μ Ci/ml of [³⁵S]methionine (ICN Biomedicals) for 60 min prior to harvesting cells as described above. Incorporation of [³⁵S]methionine into protein was determined by precipitation with trichloroacetic acid and scintillation counting.

m⁷GTP-Sepharose affinity isolation of eIF4E and associated factors. For the isolation of eIF4E and associated proteins, cell extracts of equal protein concentrations were subjected to m⁷GTP-Sepharose chromatography (Amersham

Biosciences, United Kingdom) and the resin washed twice with buffer B (20 mM morpholinopropanesulfonic acid-KOH, pH 7.4, 25 mM KCl, 2 mM $C_4H_6MgO_4$, 2 mM benzamidine, 2 mM 2-mercaptoethanol, 0.1 mM GTP, and 0.25% [vol/vol] Igepal). Recovered protein was eluted directly into sample buffer.

Immunoblotting and antibodies. Cell lysates adjusted to contain equal amounts of protein or obtained from m^7 GTP-Sepharose affinity isolation were subjected to sodium dodecyl sulfate-polyacrylamide gel electrophoresis (SDS-PAGE) and transferred to a polyvinylidene difluoride (PVDF) membrane (Amersham Biosciences, United Kingdom), and proteins were visualized with the antibodies described below. Appropriate secondary antibodies conjugated to horseradish peroxidase were used to visualize antibody complexes with enhanced chemiluminescence reagents (Perbio, United Kingdom). Polyclonal rabbit antibodies against epitopes in the C terminus of eIF4GI (residues 1179 to 1206), the N terminus of eIF4GI (residues 43 to 62), eIF4E (residues 203 to 217), and PABP1 (residues 413 to 434) have been previously described (8, 12). Rabbits were immunized with the following peptides or bacterially expressed proteins to raise polyclonal antibodies against the N terminus of eIF4GI (residues 175 to 200; KRERKTIRIRDPNQGGKDITEEIMS), against eIF4GII (residues 183 to 419; QLP.TPP), and against eIF4A (residues 348 to 369; DLPANRENYI HRTGRGGRFRGK). All peptide antisera were isolated from crude serum by affinity chromatography with the corresponding peptide using the SulfoLink kit (Perbio, United Kingdom) according to the manufacturer's instructions. The anti-Myc 4A6 monoclonal antibody was purchased from Upstate, and the anti- β -actin polyclonal antibody was from Sigma (United Kingdom). Polyclonal antibodies to 4E-BP1, phospho-4E-BP1, total eIF2 α , phospho-eIF2 α , and phospho-eIF4GI were from Cell Signaling Technology (United Kingdom). In all cases, care was taken to ensure that detection was within the linear response of the individual antiserum to the protein.

Immunofluorescence microscopy. HeLa cells, seeded on glass coverslips in six-well plates and transfected as described above, were prepared for immunofluorescence microscopy by fixation in 4% (wt/vol) paraformaldehyde in PBS, pH 7.4, for 15 min and permeabilized in PBS containing 0.1% (vol/vol) Triton X-100 for 8 min. Following blocking, eIF4GI was detected with the C-terminus-specific antibody, followed by swine antirabbit immunoglobulin G conjugated to tetramethyl rhodamine isocyanate (Dako, United Kingdom), as previously described (12). Actin was detected by phalloidin conjugated to fluorescein isothiocyanate (FITC) (Sigma, United Kingdom), while nuclei were stained with 4',6'-diamidino-2-phenylindole hydrochloride (Sigma, United Kingdom). Cells were analyzed using a Zeiss Axiocap II microscope, as previously described (12).

Statistical analysis of data. For dual-luciferase and quantitative PCR experiments, data were collected from at least three independent experiments with assays performed in duplicate. For [35 S]methionine incorporation into protein, data were collected from two independent experiments, with each assay performed in triplicate. Each chart shows the mean of these values, with error bars representing the standard error of the mean. Unpaired two-way *t* tests were performed using GraphPad Prism version 4.01 for Windows (www.graphpad.com).

RESULTS

The eIF4GI promoters are used with different efficiencies in human cell lines. Recent work has identified three promoters (α , β , and γ) (Fig. 1A) in the eIF4GI gene locus, with alternative splicing of the first eight exons giving rise to at least seven different mRNA species (Fig. 1B) (10). The mRNAs transcribed from the α and β promoters encode all possible eIF4GI proteins, whereas the single mRNA arising from the γ promoter encodes the isoform lacking the PABP-binding site (eIF4GIa). To measure the usage of the different eIF4GI promoters in different human cell lines, we have developed a quantitative RT-PCR assay. Total mRNA was reverse transcribed from three different cell lines (cervical carcinoma [HeLa], embryonic kidney cells [HEK293], and mammary carcinoma [MCF7]) (Fig. 1C), and the resulting cDNAs were amplified in the presence of the double-stranded DNA binding dye, SYBR Green. Using a reference plasmid containing a single copy of each amplicon in the same assay enabled the relative abundances of the amplicons in cellular mRNA to be determined compared to the abundance of total eIF4GI

mRNA. In all cases, controls were carried out to ensure only spliced mRNA was being amplified and not unspliced RNA or genomic DNA. It must be noted that in all these assays, the total amount of mRNA quantified from the individual promoters always exceeded that of the "total" eIF4GI amplicon; this is most likely due to the additional transcripts detected not being full-length mRNAs. Figure 1C shows that the α and β promoters are used to transcribe around 50 to 60% of eIF4GI mRNA, while the γ promoter contributes only about 5 to 10% in HeLa and HEK293 cells. In MCF7 cells, the β promoter appeared to be used preferentially; however, this value always exceeded that obtained for total eIF4GI mRNA (Fig. 1C), possibly reflecting the presence of truncated transcripts in this cell line.

The five isoforms of the eIF4GI protein arising through alternative translation initiation can be detected without in vitro proteolytic cleavage. With the discovery of the longest possible open reading frame of eIF4GI mRNA (7, 9), five protein variants of eIF4GI were found to exist in cells, generated by alternative translation initiation at various AUG codons (Fig. 1D). It has been reported that IRES sequences are present in the different eIF4GI mRNA species (9, 10, 15, 16), and it is possible that these are also being utilized in these cell lines. Previous techniques to resolve the different variants of eIF4GI and eIF4GII from cell extracts relied on proteases to bifurcate eIF4GI (7, 9). However, we have been able to use precast 4% Novex Tris-glycine gels (Invitrogen) and immunoblotting with specific antisera to resolve the eIF4GI isoforms directly from cell extracts (Fig. 1E). Using the scheme designated in reference 7, the two longest isoforms (eIF4GI_f and eIF4GI_e) were the most abundant in the three human cell lines examined, with the shortest isoform being less plentiful. This correlates with the greater amounts of transcripts from the α and β promoters (Fig. 1B and C). Immunoblotting for eIF4GI phosphorylated at Ser1148 (48) indicated that all the isoforms of eIF4GI were phosphorylated to a similar extent during logarithmic growth in the different cell types studied.

Plasmid-derived siRNA can be used to knock down eIF4GI mRNA and protein expression in HeLa cells. To investigate whether the different eIF4GI isoforms have different translational activities and binding partners, we used three siRNAs to reduce the expression of endogenous eIF4GI in HeLa cells (Fig. 2A). To first enable the fidelity of silencing to be measured, HeLa cells were transfected with vectors expressing the three different siRNA hairpins alongside a reporter construct (psiCHECK-2; Promega) expressing *Renilla* luciferase mRNA fused to the eIF4GI N-terminal RNA sequence. At 48 h after transfection, a dual-luciferase assay was used to determine the amount of *Renilla* luciferase in the cells relative to expression of control firefly luciferase transcribed from the same plasmid (Fig. 2B). These data show that transfecting HeLa cells with vectors expressing three different siRNA hairpins that target the 5' end of the eIF4GI mRNA caused a similar significant ($P < 0.001$) reduction in the levels of *Renilla* luciferase (Fig. 2B). This down-regulation of *Renilla* luciferase expression was not observed with the vector backbone alone (empty), a vector expressing a random siRNA hairpin (siNEG), or vectors expressing siRNA hairpins containing mismatches to the eIF4GI sequence (Fig. 2A). This eliminates the possibility of nonspecific micro-RNA effects being responsible for changes

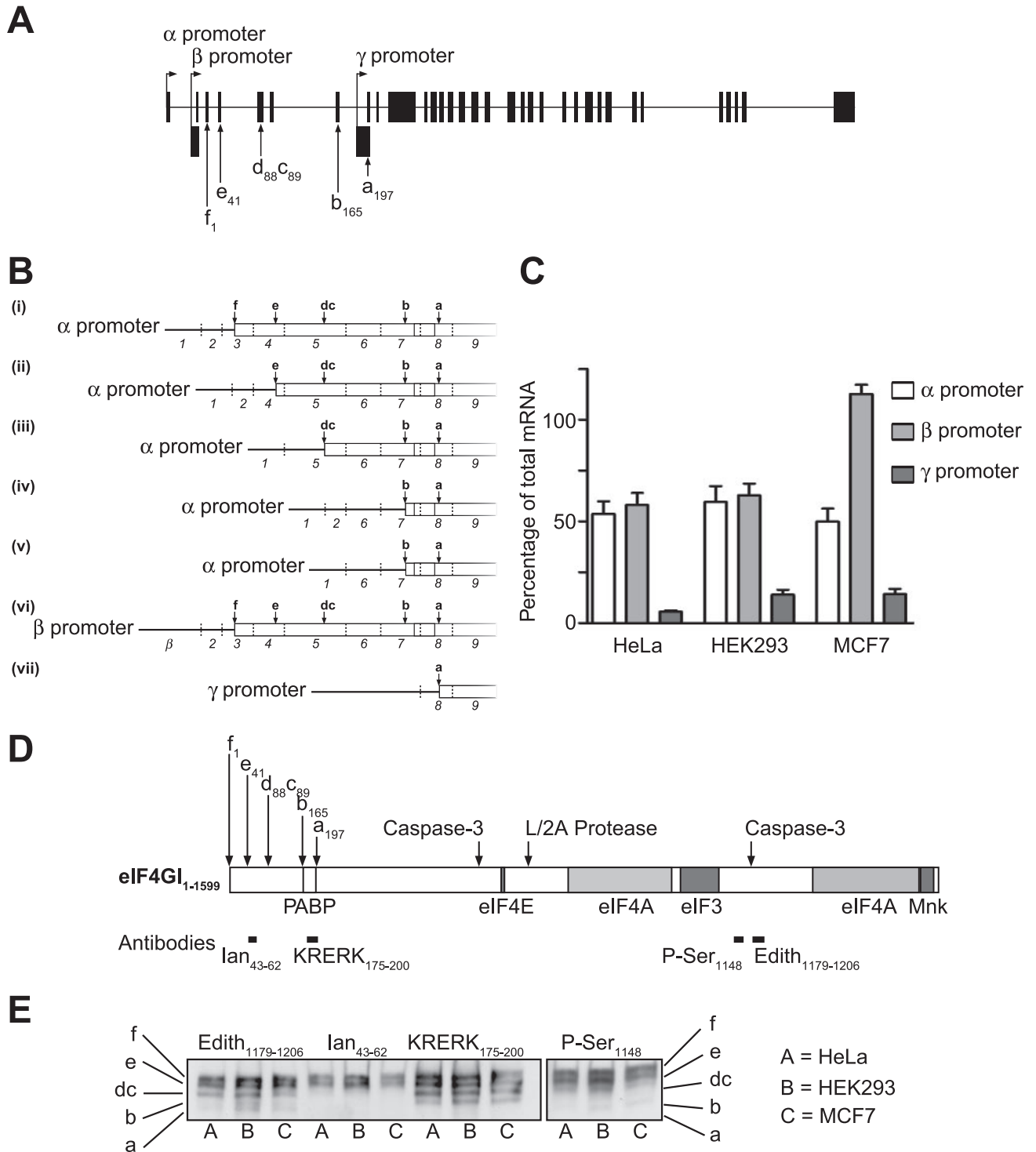


FIG. 1. The three eIF4GI promoters are used with different efficiencies in HeLa cells. **A.** Diagrammatic representation of the eIF4GI gene locus, showing the locations of the three promoters, designated α , β , and γ . Coding exons are shown in gray, and noncoding exons are shown in black. **B.** Diagrammatic representation of the eIF4GI mRNAs showing alternative splice variants generated from the different promoters (adapted from reference 10). **C.** Total RNA from the cell types shown was reverse transcribed and then amplified with primers specific to eIF4GI mRNAs. To quantify mRNAs arising from the α promoter, a primer pair that amplified only sequences containing exon 1 was created. The amplicon to quantify the mRNAs arising from the β promoter utilized a forward primer with complementarity to the β exon and a reverse primer specific for exon 3, while the γ promoter activity was quantified with a primer pair that amplified mRNAs containing exons γ and 9. Finally, a forward primer specific for exon 28 and a reverse primer complementary to exon 29 were used to quantify the total amount of eIF4GI mRNA in cells. Values obtained by quantitative RT-PCR were normalized to those obtained from an amplicon which detected all eIF4GI mRNA. Data were collected from three independent experiments, with assays each performed in triplicate, and error bars represent the standard errors of the means. **D.** Schematic representation of the eIF4GI protein. This figure shows the sites of alternative translation initiation, binding sites of other components of the translation initiation machinery (7, 10, 36), and epitopes used to generate antisera used in these studies. Sites of cleavage by caspase-3 and the picornaviral (L/2A) proteases are indicated. **E.** Equal amounts of extract from the cell types indicated were subjected to SDS-PAGE using 4% acrylamide precast gels and proteins transferred to PVDF. The membrane was then probed with the antibodies shown to visualize the eIF4GI isoforms (indicated on the left and right of the figure).

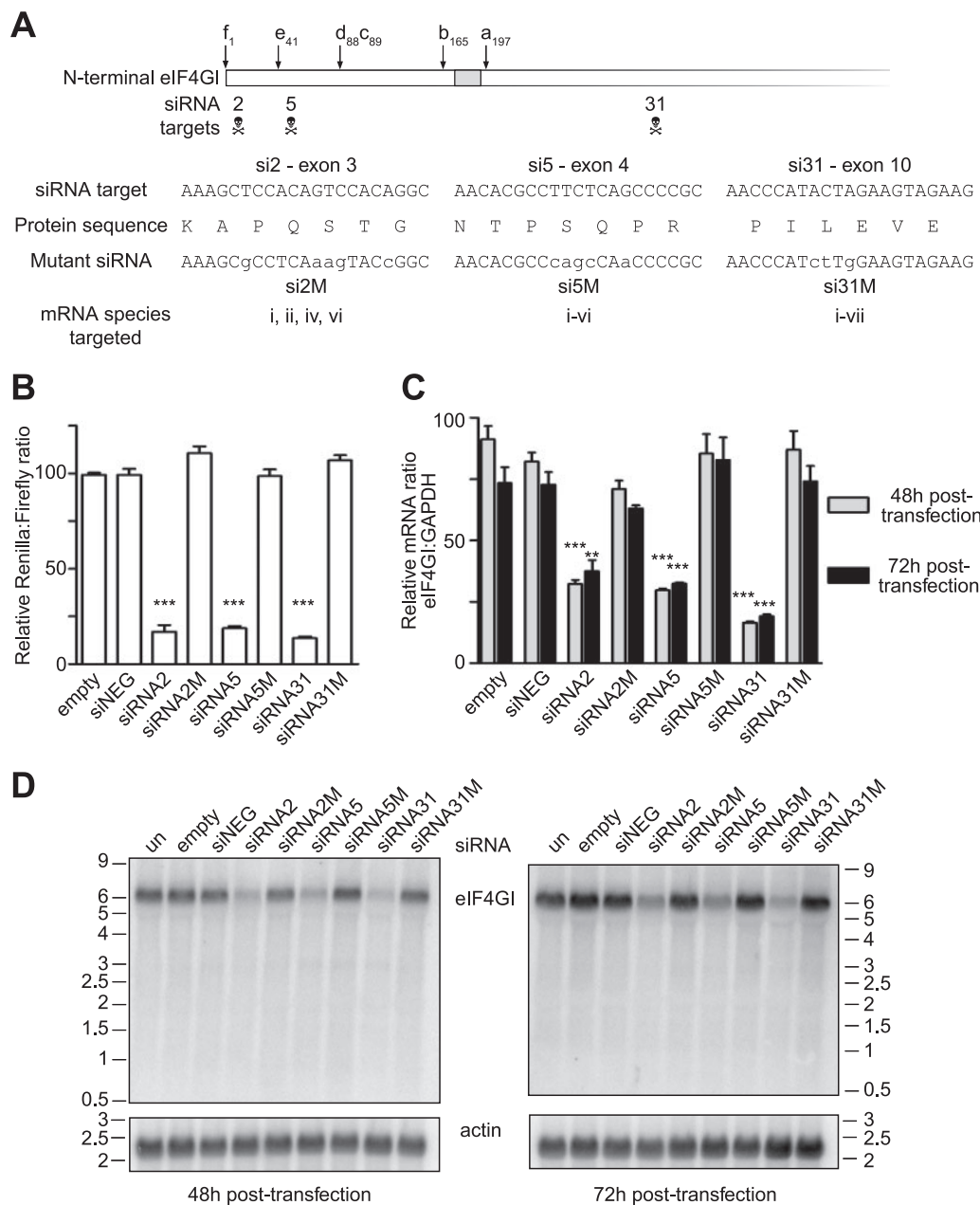


FIG. 2. Plasmid-derived siRNA can be used to knock down eIF4GI mRNA in HeLa cells. A. Three siRNA target sites were identified in the N terminus of the eIF4GI sequence, and corresponding oligonucleotides (si2, si5, and si31) were inserted into the pSilencer 3.0 H1 plasmid (Ambion). Mutated, control versions of each siRNA (si2M, si5M, and si31M) were also created that contained at least three mismatches to the center of the target site. B. siRNAs directed against eIF4GI specifically inhibit the expression of a *Renilla* luciferase mRNA fused to the eIF4GI N-terminal RNA sequence eIF4GI in the psiCHECK-2 vector. Dual-luciferase assays were performed on HeLa cell extracts prepared after 48 h of transfection, and the *Renilla* luciferase activity was normalized to firefly luciferase expressed from the same plasmid. Each variable was compared with data from cells transfected with the plasmid expressing a negative control siRNA (siNEG); ***, $P < 0.001$; $n = 3$, with error bars representing the standard errors of the means. C. HeLa cells were transfected with siRNA-expressing plasmids for the times shown, and total RNA was extracted and reverse transcribed, as described. The presence of eIF4GI or GAPDH mRNA was measured by quantitative RT-PCR. Each variable was compared as described for panel B; ***, $P < 0.001$; **, $P < 0.01$; $n = 3$, with error bars representing the standard errors of the means. D. Total RNA from HeLa cells, transfected with the indicated plasmids for the times shown, was subjected to denaturing agarose gel electrophoresis in the presence of formaldehyde. RNA was transferred to nitrocellulose and then probed with a radiolabeled, single-stranded DNA specific for the C terminus of eIF4GI. The blot was subsequently re-probed with a radiolabeled probe specific for β -actin.

in *Renilla* luciferase, and thus eIF4GI, levels (50). Having shown that this effect was specific for the eIF4GI sequence, we isolated total RNA from HeLa cells transfected for 48 h or 72 h with either control vectors or the siRNA-expressing plasmids. The siRNA-mediated knockdown of eIF4GI was measured by a quantitative RT-PCR assay using the amplicon to determine total eIF4GI mRNA levels relative to GAPDH mRNA. When expressed as a ratio, these data show that relative to results

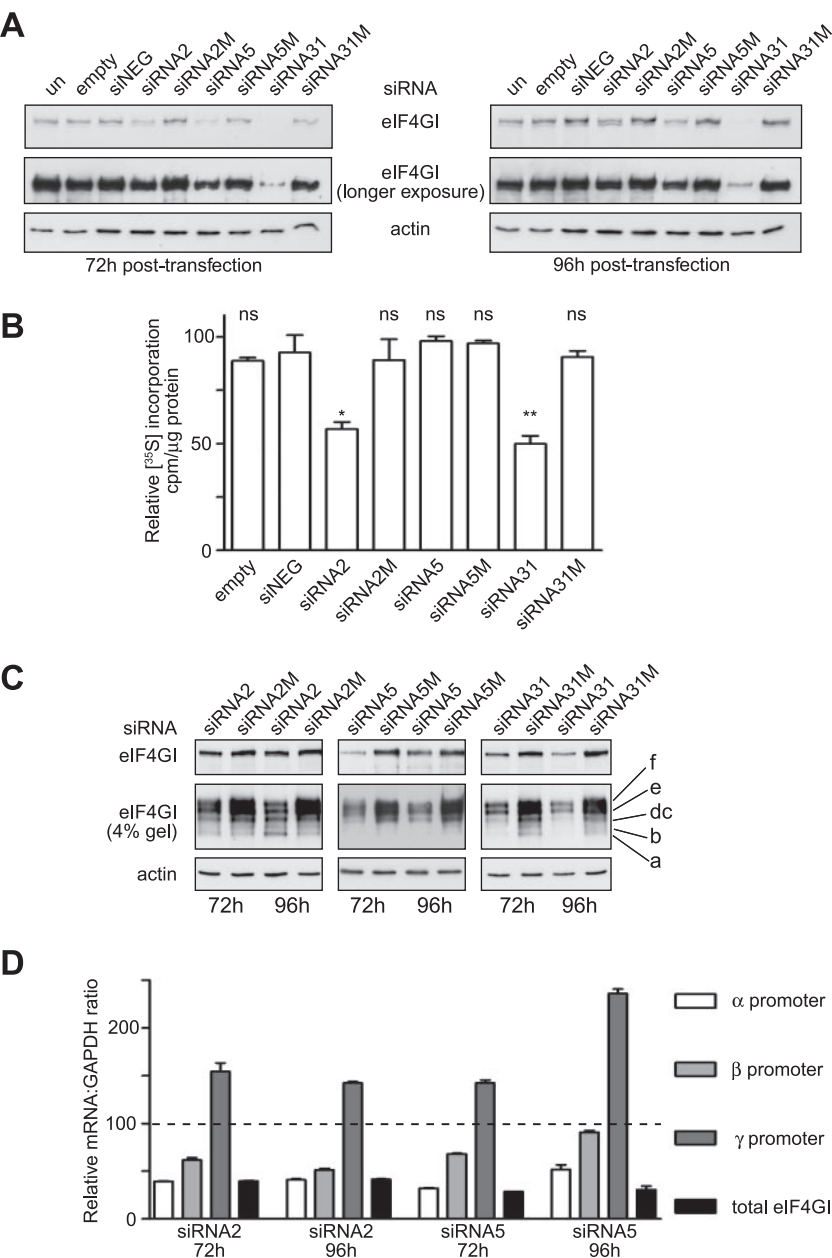


FIG. 3. Silencing of eIF4GI mRNA with alternative siRNAs has differing effects on eIF4GI protein expression and translation rates. **A.** Extracts prepared from HeLa cells after transfection for 72 h (left panel) or 96 h (right panel) with the siRNA plasmids indicated were subjected to SDS-PAGE, and proteins were transferred to PVDF, with eIF4GI and actin visualized by immunoblotting. un refers to untransfected cells, and empty refers to cells transfected with the vector alone. **B.** Prior to the harvest after 96 h of transfection, cells were incubated with [^{35}S]methionine for 1 h, extracts prepared, and the incorporation of radioactive methionine into protein determined as described in the text (expressed as cpm/ μg protein). *, $P < 0.05$; **, $P < 0.01$; ns, not significant, $P = >0.05$; $n = 3$, with error bars representing the standard errors of the means. **C.** Equal amounts of extract from HeLa cells transfected for 72 h or 96 h with the indicated siRNA plasmids were resolved by SDS-PAGE using 10% acrylamide gels (upper and lower panels) of 4% acrylamide precast gels (middle panel). eIF4GI was visualized by immunoblotting, as described, and the migration of the different isoforms is indicated on the right. **D.** To determine promoter activity in cells transfected with siRNA2 and siRNA5, total RNA was obtained from cells transfected for the times indicated and subjected to reverse transcription. Quantitative RT-PCR was performed to amplify sequences derived from each promoter for total eIF4GI mRNA and for GAPDH mRNA. The values obtained are expressed relative to the amounts of each amplicon present in untransfected cells (set at 100). Data were collected from three independent experiments, with assays each performed in triplicate, and error bars represent the standard errors of the means.

with the random siRNA hairpin (siNEG), eIF4GI mRNA was efficiently targeted in this system (Fig. 2C). This result was further confirmed by Northern blotting using a radiolabeled cDNA probe to the 3' end of eIF4GI (Fig. 2D, lanes 4, 6, and

8). To allow the eIF4GI protein to turn over following the reduction in mRNA levels, cell extracts were made 72 h and 96 h after transfection. Immunoblotting using the antibody raised against a C-terminal peptide of eIF4GI demonstrated

that siRNA31 was by far the most potent at reducing eIF4GI protein (Fig. 3A). Semiquantitative densitometrical analyses of eIF4GI expression (versus actin levels) showed that siRNA31 reduced levels of the eIF4GI protein to less than $10\% \pm 3\%$ ($n = 3$) of that presented in the untransfected control at both times. The efficacy of siRNA31 probably reflects the fact that it targets all eIF4GI-encoding mRNA species (Fig. 2A).

Decreased levels of eIF4GI protein expression result in a partial reduction in translation rates. To determine the effect of reducing eIF4GI protein levels on translation rates, cells were pulse-labeled with [35 S]methionine as described above. Figure 3B shows that when assayed after 96 h of transfection with the siRNA2 and -31-expressing plasmids, there was a significant, but incomplete, reduction in translation rates, reflecting a shift of ribosomes from polysomes to monosomes, indicative of a possible disruption of the initiation of translation (T. M. Hinton et al., submitted). Similar but less potent effects were observed at 72 h after transfection, while analysis of the proteome of siRNA31-transfected cells showed that there were also qualitative changes in protein synthesis at later times (data not shown). Surprisingly, these effects were not seen with siRNA5 (Fig. 3B), even though levels of eIF4GI were reduced by $55\% \pm 5\%$ ($n = 3$) (Fig. 3A). Further work was clearly required to determine why the alternative siRNAs differed in their ability to reduce eIF4GI levels and translation rates (see below).

The reduction in translation rates, to around 50% of that in untransfected cells, is much lower than might be expected considering the extent of the reduction in eIF4GI levels at 96 h (for si2, $50\% \pm 7\%$; for si5, $55\% \pm 5\%$; for si31, $90\% \pm 3\%$ [$n = 3$]) (Fig. 3A). However, this may reflect that ongoing translation involving recycling of ribosomes on a single mRNA is less dependent upon eIF4G (27, 39) or that there is a certain threshold where the amount of eIF4GI is sufficient for translation to be maintained. Alternatively, the less-abundant isoform of eIF4G, eIF4GII, may be able to compensate for the lack of eIF4GI under these conditions. To address this in more detail, the expression of the different eIF4GI isoforms during siRNA-mediated knockdown was examined in more depth by electrophoresis of extracts on 4% acrylamide gels (Fig. 3C). As expected, siRNA31, which is complementary to a sequence in exon 10 and targets all eIF4GI mRNA species, resulted in a reduction of all protein isoforms to a similar extent. However, when extracts from siRNA2- or siRNA5-transfected cells were examined, changes in the levels of different eIF4GI isoforms were observed, especially at 96 h. As predicted, cells transfected with siRNA5 (which targets exon 4) for 96 h showed a marked decrease in the level of eIF4GIf, with reduced expression of eIF4GIe, while eIF4GIdc was maintained relative to the other isoforms (Fig. 3C). This could in part explain why the translation rate was maintained in cells transfected with siRNA5, since the amount of eIF4GIe and eIF4GIdc in these cells may be sufficient to keep total eIF4GI levels above a critical threshold. Surprisingly, in cells transfected with siRNA2, which targets exon 3 (Fig. 2A), we observed an increase in protein expression of the shortest (eIF4GIa) isoform after 96 h of transfection. Since translation was still partially inhibited under these conditions (Fig. 3B), these data indicate that in contrast to eIF4GIdc, eIF4GIa is less able to complement the loss of the other eIF4GI isoforms, even when expressed at

elevated levels. To address whether this consistent finding reflected changes in levels of mRNAs arising from the different eIF4GI promoters, quantitative RT-PCR was used to measure these mRNA populations, total eIF4GI mRNA, and GAPDH mRNA in cells transfected with siRNA2 or -5 for 72 or 96 h, and then levels were normalized to mRNA levels in untransfected cells (set at 100; Fig. 3D). These data show that there was a reduction in the levels of mRNA from the α and β promoters, although by 96 h of transfection with siRNA5, the levels of mRNA arising from the β promoter were returning to normal. Although it was more marked in cells transfected with siRNA5 than in those transfected with siRNA2, we consistently observed an increase in transcript levels arising from the γ promoter. Since there was no concomitant increase in eIF4GIa protein levels in the case of siRNA5 (Fig. 3C), these data suggest the possibility of translational activation of the γ mRNA in response to siRNA2 for 96 h, possibly via the eIF4GI IRES sequence that resides in this transcript (10, 26).

Decreased expression of eIF4GI promotes changes in other components of the translation machinery and a reduction in active eIF4F complexes. To determine what effect the loss of eIF4GI had on other components of the translation initiation machinery, equal amounts of extracts prepared from cells transfected with siRNA2, siRNA5, or siRNA31 for 72 h or 96 h were resolved by SDS-PAGE and proteins visualized by immunoblotting. A reciprocal effect on eIF4G expression has been reported when eIF4E levels were reduced in HeLa cells using antisense RNA (13), suggesting that there may be some sort of coregulation of these two initiation factors. As shown in Fig. 4A, depletion of eIF4GI with any of these siRNAs had little impact on the total levels of PABP or eIF4A. However, levels of eIF4GII and eIF4E were consistently reduced in cells transfected with siRNA31 (Fig. 4A, right panel). This was not observed with siRNA5 (Fig. 4A, middle panel), suggesting that at least part of the lack of effect on translation rates under these conditions may reflect a compensatory effect of eIF4GII or the maintained presence of eIF4GIe and eIF4GIdc. While the phosphorylation of the α subunit of eIF2 at Ser51 was not reproducibly increased with any of the siRNAs, the phosphorylation status of the inhibitory eIF4E binding protein, 4E-BP1, showed differences in cells transfected with the different siRNAs. Relative to control siRNAs, with siRNA2 (left panel) and siRNA31 (right panel), immunoblotting with anti-eIF4E-BP1 antiserum suggested that the protein was markedly dephosphorylated at 96 h, going from the predominantly hyperphosphorylated (γ) to the hypophosphorylated (α) form. These data were confirmed by using antiserum which recognizes 4E-BP1 phosphorylated on Thr70 (Fig. 4A) and Ser65 (data not shown), events associated with its release from eIF4E (17). In contrast, this was seen to a lesser extent with siRNA5 (middle panel); in conjunction with the maintained expression of eIF4GII and eIF4Gdc, this may also impact on translation rates in these cells (17, 36). As expected, isolation of eIF4E and associated proteins by m^7 GTP-Sepharose chromatography showed that the reduction of total eIF4GI levels also caused a decrease in eIF4GI, PABP, and eIF4A copurified as part of the eIF4F complex, with a concomitant increase in recovery of 4E-BP1 (Fig. 4B). This effect was observed with siRNA2 (right panel) but was most dramatic with siRNA31 (left panel), where levels of eIF4GI were reduced to a greater extent. These

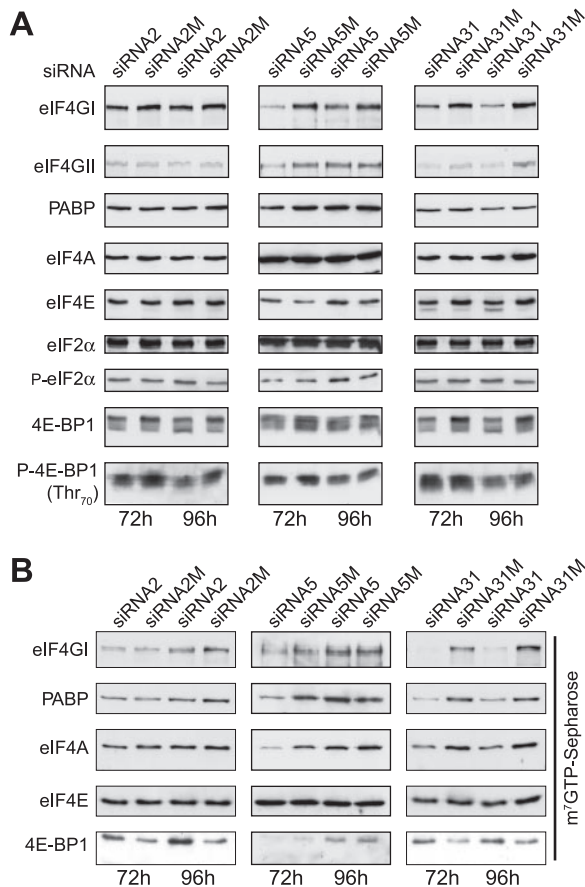


FIG. 4. Silencing of eIF4GI also results in reduced levels of eIF4E and the dephosphorylation of 4E-BP1. A. Equal amounts of cell extract from HeLa cells transfected with the indicated siRNA plasmids for 72 h or 96 h were subjected to SDS-PAGE and the indicated proteins visualized by immunoblotting. B. Aliquots of extracts containing equal amounts of protein were subjected to m⁷GTP-Sepharose affinity chromatography to recover eIF4E and associated factors. Proteins were resolved by SDS-PAGE and visualized by immunoblotting using the antisera indicated. These data are from a single experiment but are representative of those obtained in at least three separate experiments.

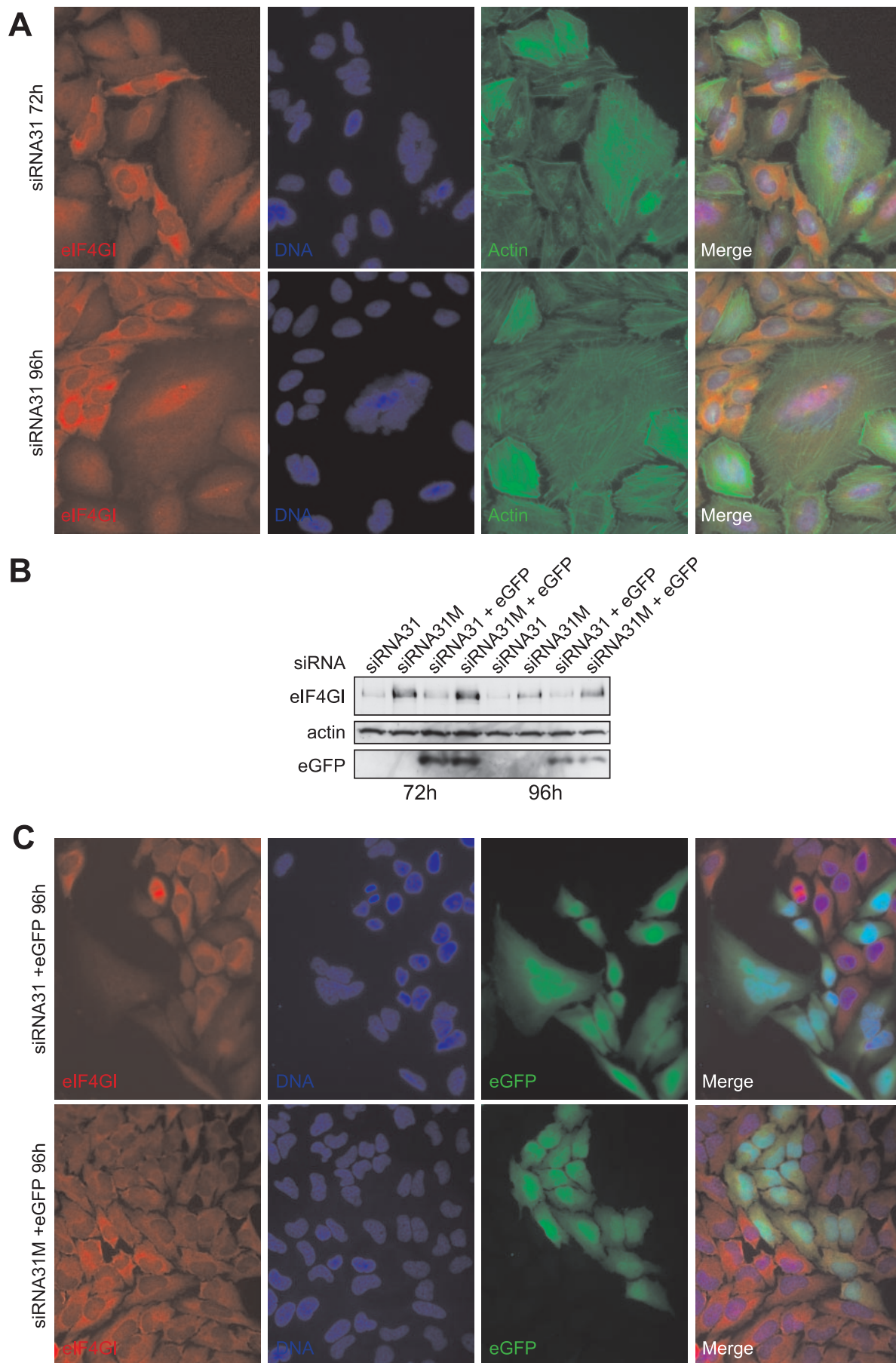
findings of reduced levels but not complete absence of eIF4F correlate well with the reduced translation rates observed in cells transfected with siRNA2 and -31 (Fig. 2A). In contrast, with siRNA5, the association of eIF4G, PABP, and eIF4A with eIF4E was not decreased, suggesting that eIF4F levels were maintained. In addition, at 96 h, the binding of 4E-BP1 to eIF4E was not increased over that observed with the control siRNA (middle panel), consistent with a lack of effect of siRNA5 on 4E-BP1 phosphorylation (Fig. 4A) and with the lack of effects on translation rates in these cells (Fig. 3B).

Cells depleted of eIF4GI exhibit a multinucleated morphology. To complement the biochemical analysis, we also wanted to determine the effects on morphology when cells were depleted of eIF4GI. Accordingly, HeLa cells were transfected with the plasmid encoding siRNA31 for 72 h or 96 h (only half the amount of siRNA plasmid was used here in order to be able to distinguish transfected from untransfected cells) and prepared for immunofluorescence microscopy as described.

eIF4GI was subsequently detected using a C-terminus-specific, affinity-purified antibody (12). As shown in Fig. 5A and in agreement with our previous studies (12, 33), while some eIF4GI resides in the nucleus, the staining pattern for eIF4GI in untransfected cells was predominantly cytoplasmic, with the majority of eIF4GI localized to the perinuclear region. However, in those cells which had reduced levels of eIF4GI, the staining pattern was more nuclear, possibly reflecting differential turnover rates of cytoplasmic and nuclear pools of eIF4GI. One of the most striking phenotypes observed in some cells depleted of eIF4GI, both with siRNA31 (Fig. 5A) and siRNA2 (data not shown), was that they were very large and often multinucleated, possibly reflecting an uncoupling of mitosis and cytokinesis as a consequence of reduced translation rates.

To further this work and to identify transfected cells more efficiently, we developed an alternative siRNA expression vector which also encoded enhanced green fluorescent protein (eGFP). The eGFP open reading frame, along with the cytomegalovirus promoter and simian virus 40 poly(A) signal from the vector pEGFP-N1 (Clontech, United Kingdom), were inserted into the pGEM T-easy vector (Promega, United Kingdom). The sequence encoding the H1 promoter, siRNA hairpin, and termination signal from the various pSilencer plasmids was then subcloned into this vector. Cells were then transfected for 72 h or 96 h with either of these plasmids (Fig. 5B, lanes 3, 4, 7, and 8) or the pSilencer plasmids (lanes 1, 2, 5, and 6), and the silencing of eIF4GI and expression of eGFP were monitored by immunoblotting. As shown in Fig. 5B, eGFP was efficiently expressed from these vectors without affecting the ability of the siRNA to reduce the level of eIF4GI. Therefore, asynchronous, mid-log-phase HeLa cells were transfected with these vectors and prepared for immunofluorescence microscopy (Fig. 5C). The difference in eIF4GI staining (red) is clearly evident between those cells which have been transfected with the plasmid (and therefore express eGFP [green]) and those which have not. Again, a number of cells depleted for eIF4GI and contributing to the inhibition of protein synthesis became enlarged and multinucleated. This vector was also utilized in live cell imaging, where the different events leading to multinucleation can be observed in more detail (see the supplemental material). These data show that some cells depleted for eIF4GI did not divide at all, possibly because they were unable to synthesize essential proteins required for cell cycle transition. In addition, other cells divided normally, with daughter cells then fusing before dividing again, leading to a multinucleated phenotype. In other examples, cells divided into very unequal daughter cells, the smaller of which eventually underwent apoptosis, while the larger cell survived to divide into three cells. These data confirm that perturbations in protein synthesis caused by depletion of eIF4GI, below a critical threshold, had severe effects on protein synthesis, the control of cell cycle progression, and cytokinesis.

siRNA-resistant eIF4G is incorporated into eIF4F and leads to partial restoration of translation rates. To facilitate the expression of eIF4GI cDNAs in cells in which levels of endogenous eIF4GI had been reduced, the three mismatches used to create the control siRNA (si31M) were introduced into Myc-tagged eIF4GI cDNAs (12). This rendered them siRNA resistant without changing the amino acid sequences of the eIF4GI isoforms. Other cDNAs encoding the middle caspase



cleavage fragment of eIF4GI (M-FAG) and eIF4GII cDNAs (18) were expressed without any further manipulation. Plasmids encoding siRNA31 and the resistant Myc-tagged eIF4GI isoforms (Fig. 6A) or eIF4GII (Fig. 6B) were cotransfected into HeLa cells for 96 h and the levels of endogenous and exogenous eIF4G monitored by immunoblotting. Figures 6A and B show that endogenous eIF4GI was efficiently reduced by siRNA31 (lane 2 versus lane 1), with the different, resistant isoforms of eIF4GI expressed to different levels (Fig. 6A, lanes 3 to 7), without any effect on total PABP or eIF4A. In agreement with previous data (Fig. 4A), 4E-BP1 was dephosphorylated in response to siRNA31 (lane 2 versus lane 1). When monitored with anti-eIF4GI serum, we consistently found that eIF4GIf (lane 3), eIF4GIe (lane 4), and eIF4GIdc (lane 5) were expressed at levels similar to those of the endogenous protein, while eIF4GIb (lane 6), eIF4GIa (lane 7), and MFAG (lane 8) were expressed at much higher levels, as observed previously (12). Although levels of eIF4E were decreased by siRNA31, expression of eIF4GI isoforms largely prevented this decrease (lanes 3 to 7 versus lane 2). In addition, as shown with both antiserum to the total protein and that recognizing 4E-BP1 phosphorylated at Thr70, expression of all isoforms of eIF4GI (Fig. 6A, lanes 3 to 8) or eIF4GII (Fig. 6B, lane 4 versus lane 2) resulted in the phosphorylation of 4E-BP1, albeit to differing degrees. Myc-eIF4GII was consistently expressed at levels similar to that of Myc-eIF4GIf (Fig. 6B, lane 4 versus lane 3), representing expression to a much higher level than the endogenous protein (lane 3 versus lane 1). The incorporation of each of the expressed siRNA-resistant eIF4GI proteins or eIF4GII into eIF4F complexes was also examined by m⁷GTP-Sepharose chromatography (Fig. 6A and B, lower panels). As expected, siRNA31 reduced the recovery of eIF4GI, eIF4A, and PABP in association with eIF4E (lanes 2 versus lanes 1). Coexpression of the Myc-eIF4GI proteins (Fig. 6A, lanes 3 to 8) or eIF4GII (Fig. 6B, lanes 3 and 4) resulted in the incorporation of eIF4G into eIF4F complexes to a level reflecting their total level of expression (upper panel). The recruitment of PABP into eIF4F was partially restored in cells expressing eIF4GII (Fig. 6B, lane 4) or eIF4GI with the ability to bind PABP (Fig. 6A, lanes 3 to 6). However, these data clearly show that the levels of PABP and eIF4A associated to eIF4E were not fully restored upon reintroduction of eIF4G isoforms but were increased over the levels seen when eIF4GI was depleted (Fig. 6A, lanes 3 to 8 versus lane 2, and Fig. 6B, lanes 3 and 4 versus lane 2). In contrast, those cells expressing eIF4GIa (lane 7) or M-FAG (lane 8) showed PABP levels similar to those observed in the siRNA31-transfected cells (lane 2). The recovery of eIF4A in the eIF4F complex was

increased in all the cells expressing Myc-eIF4GI, although for eIF4GIa (lane 7) and M-FAG (lane 8) this was not as great as would be predicted from their expression levels.

Translation rates were assayed in parallel by measuring the incorporation of [³⁵S]methionine into total protein and were expressed relative to the rate measured in untransfected cells (Fig. 6C). As before (Fig. 3B), siRNA31-mediated reduction of eIF4GI levels resulted in a partial inhibition of translation that was significantly prevented by coexpression of low levels of eIF4GIf (Fig. 6A, lane 3 versus lane 2; $P < 0.001$) but not back to the level obtained with the siRNA31M control. eIF4GIe (lane 4) and eIF4GIb (lane 6) were as effective as eIF4GIf (lane 3) in this response, but eIF4GIdc (lane 5) and eIF4GIa (lane 7) were significantly less able ($P < 0.005$), in spite of the latter being expressed to relatively high levels. High levels of M-FAG (lane 8) and eIF4GII (lane 9) were able to induce a small increase in the rate of translation over that in the silenced cells, but not to the level observed with eIF4If ($P < 0.05$). Although there were no obvious qualitative differences in translation assessed by SDS-PAGE, work is currently under way to establish just how the isoforms of eIF4GI and eIF4GII differ in their ability to recruit different mRNAs and proteins to active translation complexes.

DISCUSSION

Mammalian eIF4GI is a family of modular proteins, consisting of three domains of approximately 500 amino acids each (as defined by proteolytic cleavage), separated by unstructured linker regions (37, 43). eIF4GI has an important role in translation initiation, allowing multiple initiation factors to assemble at the 5' cap of an mRNA molecule, thereby promoting its recruitment by the small ribosomal subunit (reviewed in reference 37). Recent studies with *Saccharomyces cerevisiae* have also suggested that eIF4G may have an undetermined but rate-limiting function at a step downstream of 48S complex assembly in vivo (24). In spite of this knowledge, little is known about how the level of eIF4G is regulated at the transcriptional and translational levels, and IRES sequences present in the different eIF4GI mRNA species may also play a role in expression under different growth conditions (9, 10, 15, 16, 47). To address this, we have quantified eIF4GI mRNA levels from a number of mammalian cell lines. Figure 1C shows that the α and β promoters are used to transcribe around 50 to 60% of eIF4GI mRNA, while the γ promoter contributes only about 5 to 10% in HeLa and HEK293 cells. We have also shown that it is possible to resolve the eIF4GI isoforms directly from cell extracts by using 4% Novex Tris-glycine gels and immunoblotting with specific antisera (Fig. 1E). Western blotting con-

FIG. 5. HeLa cells with reduced expression of eIF4GI often show a multinucleated morphology. A. HeLa cells were grown on glass coverslips and after transfection for 72 h (top panels) or 96 h (bottom panels) with siRNA31 were processed for immunofluorescence microscopy, as described in the text. eIF4GI was detected with the C-terminus-specific antibody, followed by goat antirabbit immunoglobulin G conjugated to tetramethyl rhodamine isocyanate; actin was detected with phalloidin conjugated to FITC, while nuclei were stained with 4',6'-diamidino-2-phenylindole hydrochloride. These data are from a single experiment but are representative of those obtained in at least five separate experiments. B. HeLa cells were transfected with siRNA31 expression vectors (lanes 1, 2, 5, and 6) or siRNA31-eGFP vectors (lane 3, 4, 7, and 8) for the times indicated. Extracts were prepared, and eIF4GI, actin, and eGFP expression was monitored by SDS-PAGE and immunoblotting, as indicated. C. HeLa cells were grown on glass coverslips and after transfection for 96 h with siRNA31-eGFP (upper panels) or siRNA31M-eGFP (lower panels) were processed for immunofluorescence microscopy, as described for panel A. These data are from a single experiment but are representative of those obtained in at least three separate experiments.

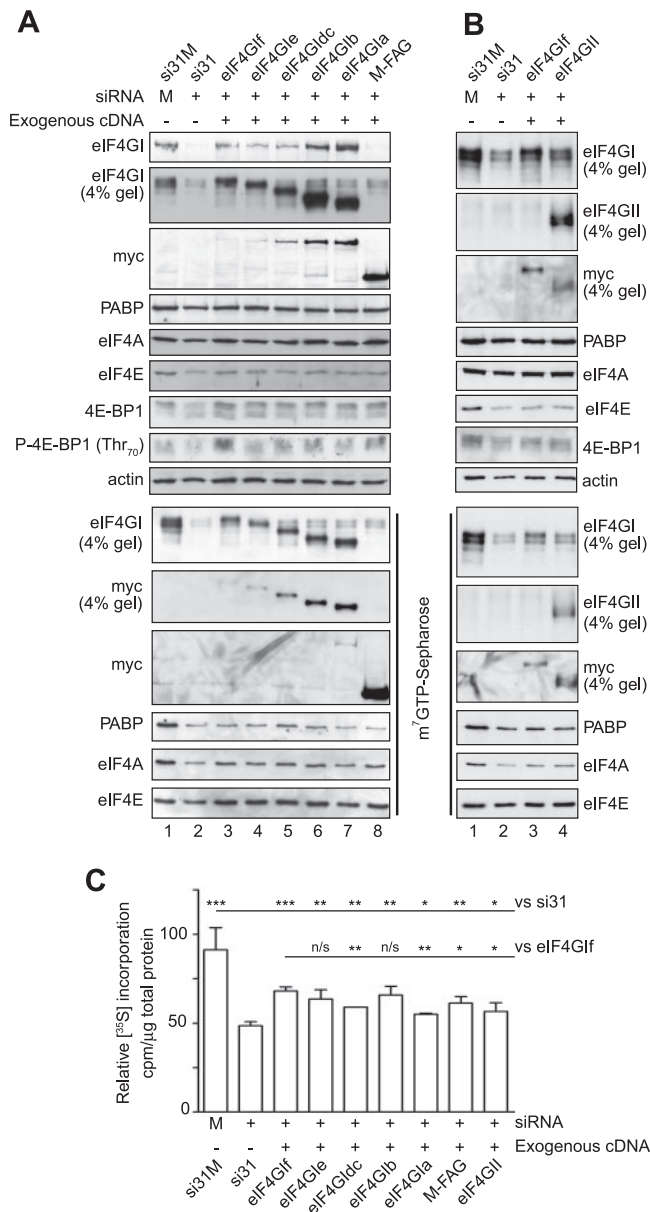


FIG. 6. Low levels of eIF4Gf are more efficient than high levels of eIF4Gla at partial restoration of translation rates following reduced expression of endogenous eIF4GI. **A** (upper). HeLa cells were cotransfected for 96 h with siRNA vectors and plasmids expressing different Myc-tagged isoforms of eIF4GI or the apoptotic cleavage fragment of eIF4G (M-FAG), as indicated. Cell extracts were prepared and aliquots containing equal amounts of total protein resolved by SDS-PAGE using 10% acrylamide gels or 4% acrylamide precast gels, as indicated. eIF4GI was visualized by immunoblotting using either anti-Myc antibody or anti-eIF4GI antiserum, and other proteins were visualized using the antisera indicated. (Lower) Aliquots of extracts containing equal amounts of protein were subjected to m⁷GTP-Sepharose affinity chromatography to recover eIF4E and associated factors. Proteins were resolved by SDS-PAGE and visualized by immunoblotting using the antisera indicated. **B** (upper). HeLa cells were cotransfected for 96 h with siRNA vectors and plasmids expressing Myc-eIF4GII, as indicated. Extracts were prepared and proteins visualized as for panel A. (Lower) Aliquots of extracts containing equal amounts of protein were subjected to m⁷GTP-Sepharose affinity chromatography to recover eIF4E and associated factors, as described above. **C.** Prior to the harvest after 96 h of transfection, cells were incubated with [³⁵S]methionine for 1 h, extracts prepared, and the incorporation of

radioactive methionine into protein determined as described in the text (expressed as cpm/μg total protein). Unpaired two-way *t* tests were performed separately, comparing eIF4Gf with si31 (***, *P* < 0.001; *n* = 3) and comparing eIF4Gf with other isoforms of eIF4GI (*, *P* < 0.05; **, *P* < 0.01; ns, *P* = >0.05; *n* = 3), with error bars representing standard errors of the means.

firming that we can resolve five isoforms of eIF4GI and that, consistent with data from K562 cells (7), eIF4Gf and eIF4Gle are the most abundant in the human lines tested (Fig. 1E). This correlated with the greater amounts of transcripts from the α and β promoters (Fig. 1B and C). Surprisingly, we found that transcript levels arising from the γ promoter increased in response to siRNA-mediated reduction of mRNA expression from the α and β promoters (Fig. 3D). Since a concomitant increase in the eIF4Gla protein level (Fig. 3C) was seen with the siRNA targeting mRNAs i to vi (Fig. 2A), these data suggest that translational activation of the γ mRNA occurs at later incubation times, possibly *via* the eIF4GI IRES sequence that resides in this transcript. Further work is under way to determine whether reduced mRNA expression from the α and β promoters occurs during mitosis, thereby explaining why eIF4GI mRNA is retained in polysomes under conditions of reduced cap-dependent translation (26, 47).

Apart from the presence of the PABP binding site (23, 42), little is known about the poorly conserved N-terminal domain differentially expressed in the eIF4GI isoforms (Fig. 1D) or how it might influence the function of the protein. The shortest isoform (designated eIF4Gla, also the first cloned [52]) lacks the sequence that interacts with PABP (Fig. 1D) but is still capable of transforming cells when overexpressed (14, 22). The eIF4E binding domain and central region are highly conserved, being essential for cap-dependent translation (35). The former undergoes a disordered-to-ordered transition when it binds eIF4E (20, 31), while the central domain shows a defined globular structure consisting of five HEAT repeats (31). The C-terminal region, which is restricted to higher eukaryotes, has recently been shown to contain two atypical HEAT domains (4) and appears to modulate translation driven by the central domain (35). Most *in vivo* experiments to determine the role for various isoforms or cleavage fragments of eIF4GI have been carried out in a background of endogenous eIF4GI expression (37). Here we have begun to address the possible roles for the individual isoforms of eIF4GI in promoting translation initiation by using siRNAs to specifically inhibit its expression. Data presented in Fig. 2 and 3 show that eIF4GI mRNA was efficiently targeted, that siRNA31 was by far the most potent at reducing eIF4GI protein levels at 72 or 96 h after transfection, and that this resulted in a significant but incomplete reduction in translation rates. With siRNA31, the 50% decrease in the translation rate was much lower than expected considering the extent of the reduction in eIF4GI (Fig. 3A), the dephosphorylation of 4E-BP1 (Fig. 4A), and the decrease in eIF4F levels (Fig. 4B). Although it could not be ascribed to changes in eIF2α phosphorylation (Fig. 4A), the incomplete inhibition could reflect that only a population of the cells was transfected under these conditions. In addition, it could also reflect that ongoing translation involving recycling

radioactive methionine into protein determined as described in the text (expressed as cpm/μg total protein). Unpaired two-way *t* tests were performed separately, comparing eIF4Gf with si31 (***, *P* < 0.001; *n* = 3) and comparing eIF4Gf with other isoforms of eIF4GI (*, *P* < 0.05; **, *P* < 0.01; ns, *P* = >0.05; *n* = 3), with error bars representing standard errors of the means.

of ribosomes on a single mRNA is less dependent upon intact eIF4G (27, 39). A recent study has shown that translation compartmentalized to the endoplasmic reticulum (ER) is resistant to cleavage of eIF4GI by Cocksackie B virus (29), raising the possibility that ongoing translation is maintained on the ER in siRNA31-treated cells, although staining of eIF4GI in the siRNA31-transfected cells does not reveal a pattern consistent with ER staining. Alternatively, it may be that there is a threshold where the amount of eIF4GI is sufficient for translation to be maintained or that the less-abundant isoform of eIF4G, eIF4GII, can compensate for eIF4GI under these conditions. While eIF4GIa levels were increased with siRNA2 treatment at 96 h (Fig. 3C), it is unlikely to be masking an effect on down-regulating translation, since a similar level of inhibition was observed with siRNA31, which had no effect on eIF4GIa levels (Fig. 3B).

In all cases, the failure to rescue translation to the control level may reflect that we are examining a mixed cell population. For instance, as shown in Fig. 5 (and reference (12)), some cells express high levels of Myc-eIF4GI, others lower levels, and others none at all, but with analysis by SDS-PAGE, we observed a reasonable, overall expression. It is also possible that not all silenced cells were cotransfected with the siRNA-resistant eIF4G cDNAs. We are currently attempting to address this by studying the rescue of translation in eGFP-positive cells sorted by fluorescence-activated cell sorting. Due to the phenotype associated with reduced expression of eIF4GI (Fig. 5), we have not been able to generate viable, stable cell lines, but attempts will be made to generate stable cell lines to allow for inducible expression of siRNAs. Another explanation could be that replacement of endogenous eIF4GI with just a single isoform was insufficient to fully recover translation rates. However, coexpression of eIF4GIf and eIF4GIe was insufficient to rescue translation rates above that seen with the individual isoforms (data not shown).

Figure 6A shows that even though the eIF4GIf isoform was the least abundantly expressed, it was relatively more efficient at restoring overall translation rates than the eIF4GII or eIF4GI isoform, which was expressed to higher levels (Fig. 6A to C). Even though the shorter, eIF4GIa isoform was expressed to the highest level and was incorporated efficiently into eIF4F complexes, we consistently found that possession of an N-terminal extension rendered eIF4GIe and eIF4GIb statistically more efficient at rescuing translation rates than eIF4GIa. Similarly, overexpression of M-FAG, the minimum fragment of eIF4GI able to participate in *in vitro* cap-dependent translation (35) and which binds to eIF4E, eIF4A, and eIF3, was unable to rescue translation to the same extent as the longest isoforms of eIF4GI, possibly reflecting the poorer incorporation of eIF4A into eIF4F complexes in these cells. The effects of reintroduction of eIF4GI cDNAs lacking partner binding sites on general protein synthesis have also been tested (Hinton et al., submitted). These data suggest that the PABP interaction site is not required for the rescue of translation, suggesting a novel function for the N-terminal extension of eIF4GI. Using the techniques developed in this study, we are currently in the process of characterizing proteins which interact with this sequence and attempting to further delineate eIF4G isoform-specific effects on cap-dependent and cap-in-

dependent mRNA translation using microarray analysis of polysome-associated mRNAs.

ACKNOWLEDGMENTS

We thank Sally Wheatley (GDSC, Sussex, United Kingdom) for advice and help with the live cell imaging.

We thank the BBSRC (United Kingdom; grant number 007593/1) for funding this work.

REFERENCES

- Abbott, C. M., and C. G. Proud. 2004. Translation factors: in sickness and in health. *Trends Biochem. Sci.* **29**:25–31.
- Avdulov, S., S. Li, V. Michalek, D. Burrichter, M. Peterson, D. M. Perlman, J. C. Manivel, N. Sonenberg, D. Yee, P. B. Bitterman, and V. A. Polunovsky. 2004. Activation of translation complex eIF4F is essential for the genesis and maintenance of the malignant phenotype in human mammary epithelial cells. *Cancer Cell* **5**:553–563.
- Bauer, C., I. Diesinger, N. Brass, H. Steinhart, H. Iro, and E. U. Meese. 2001. Translation initiation factor eIF-4G is immunogenic, overexpressed, and amplified in patients with squamous cell lung carcinoma. *Cancer* **92**:822–829.
- Bellsolell, L., P. F. Cho-Park, F. Poulin, N. Sonenberg, and S. K. Burley. 2006. Two structurally atypical HEAT domains in the C-terminal portion of human eIF4G support binding to eIF4A and Mnk1. *Structure* **14**:913–923.
- Belsham, G. J., and R. J. Jackson. 2000. Translation initiation on Picornavirus RNA, p. 869–900. *In* N. Sonenberg, J. W. B. Hershey, and M. B. Mathews (ed.), *Translational control of gene expression*. Cold Spring Harbor Laboratory Press, Cold Spring Harbor, N.Y.
- Berset, C., A. Zurbriggen, S. Djafarzadeh, M. Altmann, and H. Trachsel. 2003. RNA-binding activity of translation initiation factor eIF4G1 from *Saccharomyces cerevisiae*. *RNA* **9**:871–880.
- Bradley, C. A., J. C. Padovan, T. C. Thompson, C. A. Benoit, B. T. Chait, and R. E. Rhoads. 2002. Mass spectrometric analysis of the N-terminus of translation initiation factor eIF4G-1 reveals novel isoforms. *J. Biol. Chem.* **277**:12559–12571.
- Bushell, M., D. Poncet, W. E. Marissen, H. Flotow, R. E. Lloyd, M. J. Clemens, and S. J. Morley. 2000. Cleavage of polypeptide chain initiation factor eIF4GI during apoptosis in lymphoma cells: characterisation of an internal fragment generated by caspase-3-mediated cleavage. *Cell Death Differ.* **7**:628–636.
- Byrd, M. P., M. Zamora, and R. E. Lloyd. 2002. Generation of multiple isoforms of eukaryotic translation initiation factor 4GI by use of alternate translation initiation codons. *Mol. Cell. Biol.* **22**:4499–4511.
- Byrd, M. P., M. Zamora, and R. E. Lloyd. 2005. Translation of eukaryotic translation initiation factor 4GI (eIF4GI) proceeds from multiple mRNAs containing a novel cap-dependent internal ribosome entry site (IRES) that is active during poliovirus infection. *J. Biol. Chem.* **280**:18610–18622.
- Caron, S., M. Charon, E. Cramer, N. Sonenberg, and I. Dusanter-Fourt. 2004. Selective modification of eukaryotic initiation factor 4F (eIF4F) at the onset of cell differentiation: recruitment of eIF4GII and long-lasting phosphorylation of eIF4E. *Mol. Cell. Biol.* **24**:4920–4928.
- Coldwell, M. J., L. Hashemzadeh-Boneh, T. M. Hinton, S. J. Morley, and K. M. Pain. 2004. Expression of fragments of translation initiation factor eIF4GI reveals a nuclear localisation signal within the N-terminal apoptotic cleavage fragment N-FAG. *J. Cell Sci.* **117**:2545–2555.
- De Benedetti, A., S. Joshi-Barve, C. Rinker-Schaeffer, and R. E. Rhoads. 1991. Expression of antisense RNA against initiation factor eIF4E mRNA in HeLa cells results in lengthened cell division times, diminished translation rates and reduced levels of both eIF-4E and the p220 component of eIF-4F. *Mol. Cell. Biol.* **11**:5435–5445.
- Fukuchi-Shimogori, T., I. Ishii, K. Kashiwagi, H. Mashiba, H. Ekimoto, and K. Igarashi. 1997. Malignant transformation by overproduction of translation initiation factor eIF4G. *Cancer Res.* **57**:5041–5044.
- Gan, W., M. La Celle, and R. E. Rhoads. 1998. Functional characterization of the internal ribosome entry site of eIF4G mRNA. *J. Biol. Chem.* **273**:5006–5012.
- Gan, W., and R. E. Rhoads. 1996. Internal initiation of translation directed by the 5'-untranslated region of the mRNA for eIF4G, a factor involved in the picornavirus-induced switch from cap-dependent to internal initiation. *J. Biol. Chem.* **271**:623–626.
- Gingras, A. C., B. Raught, and N. Sonenberg. 1999. eIF4 initiation factors: effectors of mRNA recruitment to ribosomes and regulators of translation. *Annu. Rev. Biochem.* **68**:913–963.
- Gradi, A., H. Imataka, Y. V. Svitkin, E. Rom, B. Raught, S. Morino, and N. Sonenberg. 1998. A novel functional human eukaryotic translation initiation factor 4G. *Mol. Cell. Biol.* **18**:334–342.
- Gray, N. K., and M. Wickens. 1998. Control of translation initiation in animals. *Annu. Rev. Cell Dev. Biol.* **14**:399–458.
- Gross, J. D., N. J. Moerke, T. von der Haar, A. A. Lugovskoy, A. B. Sachs, J. E. McCarthy, and G. Wagner. 2003. Ribosome loading onto the mRNA

- cap is driven by conformational coupling between eIF4G and eIF4E. *Cell* **115**:739–750.
21. **Hammond, S. M., A. A. Caudy, and G. J. Hannon.** 2001. Post-transcriptional gene silencing by double-stranded RNA. *Nat. Rev. Genet.* **2**:110–119.
 22. **Hayashi, S., K. Nishimura, T. Fukuchi-Shimogori, K. Kashiwagi, and K. Igarashi.** 2000. Increase in cap- and IRES-dependent protein synthesis by overproduction of translation initiation factor eIF4G. *Biochem. Biophys. Res. Commun.* **277**:117–123.
 23. **Imataka, H., A. Gradi, and N. Sonenberg.** 1998. A newly identified N-terminal amino acid sequence of human eIF4G binds poly(A)-binding protein and functions in poly(A)-dependent translation. *EMBO J.* **17**:7480–7489.
 24. **Jivotovskaya, A. V., L. Valasek, A. G. Hinnebusch, and K. H. Nielsen.** 2006. Eukaryotic translation initiation factor 3 (eIF3) and eIF2 can promote mRNA binding to 40S subunits independently of eIF4G in yeast. *Mol. Cell. Biol.* **26**:1355–1372.
 25. **Johannes, G., M. S. Carter, M. B. Eisen, P. O. Brown, and P. Sarnow.** 1999. Identification of eukaryotic mRNAs that are translated at reduced cap-binding complex eIF4F concentrations using a cDNA microarray. *Proc. Natl. Acad. Sci. USA* **96**:13118–13123.
 26. **Johannes, G., and P. Sarnow.** 1998. Cap-independent polysomal association of natural mRNAs encoding c-myc, Bip, and eIF4G conferred by internal ribosome entry sites. *RNA* **4**:1500–1513.
 27. **Keiper, B. D., and R. E. Rhoads.** 1997. Cap-independent translation initiation in *Xenopus* oocytes. *Nucleic Acids Res.* **25**:395–402.
 28. **Kim, C. Y., K. Takahashi, T. B. Nguyen, J. K. Roberts, and C. Webster.** 1999. Identification of a nucleic acid binding domain in eukaryotic initiation factor eIFiso4G from wheat. *J. Biol. Chem.* **274**:10603–10608.
 29. **Lerner, R. S., and C. V. Nicchitta.** 2006. mRNA translation is compartmentalized to the endoplasmic reticulum following physiological inhibition of cap-dependent translation. *RNA* **12**:775–789.
 30. **Lomakin, I. B., C. U. Hellen, and T. V. Pestova.** 2000. Physical association of eukaryotic initiation factor 4G (eIF4G) with eIF4A strongly enhances binding of eIF4G to the internal ribosomal entry site of encephalomyocarditis virus and is required for internal initiation of translation. *Mol. Cell. Biol.* **20**:6019–6029.
 31. **Marcotrigiano, J., I. B. Lomakin, N. Sonenberg, T. V. Pestova, C. U. Hellen, and S. K. Burley.** 2001. A conserved HEAT domain within eIF4G directs assembly of the translation initiation machinery. *Mol. Cell* **7**:193–203.
 32. **Mathews, M. B., N. Sonenberg, and J. W. B. Hershey.** 2000. Origins and principles of translational control, p. 1–31. *In* N. Sonenberg, J. W. B. Hershey, and M. B. Mathews (ed.), *Translational control of gene expression*. Cold Spring Harbor Laboratory Press, Cold Spring Harbor, N.Y.
 33. **McKendrick, L., E. Thompson, J. Ferreira, S. J. Morley, and J. D. Lewis.** 2001. Interaction of eukaryotic translation initiation factor 4G with the nuclear cap-binding complex provides a link between nuclear and cytoplasmic functions of the m⁷ guanosine cap. *Mol. Cell. Biol.* **21**:3632–3641.
 34. **Meric, F., and K. K. Hunt.** 2002. Translation initiation in cancer: a novel target for therapy. *Mol. Cancer Ther.* **1**:971–979.
 35. **Morino, S., H. Imataka, Y. V. Svitkin, T. V. Pestova, and N. Sonenberg.** 2000. Eukaryotic translation initiation factor 4E (eIF4E) binding site and the middle one-third of eIF4GI constitute the core domain for cap-dependent translation, and the C-terminal one-third functions as a modulatory region. *Mol. Cell. Biol.* **20**:468–477.
 36. **Morley, S. J.** 2001. The regulation of eIF4F during cell growth and cell death. *Prog. Mol. Subcell. Biol.* **27**:1–37.
 37. **Morley, S. J., M. J. Coldwell, and M. J. Clemens.** 2005. Initiation factor modifications in the preapoptotic phase. *Cell Death Differ.* **12**:571–584.
 38. **Morley, S. J., P. S. Curtis, and V. M. Pain.** 1997. eIF4G: Translation's mystery factor begins to yield its secrets. *RNA* **3**:1085–1104.
 39. **Novoa, I., and L. Carrasco.** 1999. Cleavage of eukaryotic translation initiation factor 4G by exogenously added hybrid proteins containing poliovirus 2Apro in HeLa cells: effects on gene expression. *Mol. Cell. Biol.* **19**:2445–2454.
 40. **Ohlmann, T., D. Prevot, D. Decimo, F. Roux, J. Garin, S. J. Morley, and J. L. Darlix.** 2002. In vitro cleavage of eIF4GI but not eIF4GII by HIV-1 protease and its effects on translation in the rabbit reticulocyte lysate system. *J. Mol. Biol.* **318**:9–20.
 41. **Pestova, T. V., C. U. T. Hellen, and I. N. Shatsky.** 1996. Canonical eukaryotic initiation factors determine initiation of translation by internal ribosome entry. *Mol. Cell. Biol.* **16**:6859–6869.
 42. **Piron, M., P. Vende, J. Cohen, and D. Poncet.** 1998. Rotavirus RNA-binding protein NSP3 interacts with eIF4GI and evicts the poly(A) binding protein from eIF4F. *EMBO J.* **17**:5811–5821.
 43. **Prevot, D., J. L. Darlix, and T. Ohlmann.** 2003. Conducting the initiation of protein synthesis: the role of eIF4G. *Biol. Cell* **95**:141–156.
 44. **Pyronnet, S., J. Dostie, and N. Sonenberg.** 2001. Suppression of cap-dependent translation in mitosis. *Genes Dev.* **15**:2083–2093.
 45. **Pyronnet, S., H. Imataka, A. C. Gingras, R. Fukunaga, T. Hunter, and N. Sonenberg.** 1999. Human eukaryotic translation initiation factor 4G (eIF4G) recruits mnk1 to phosphorylate eIF4E. *EMBO J.* **18**:270–279.
 46. **Qin, H., B. Raught, N. Sonenberg, E. G. Goldstein, and A. M. Edelman.** 2003. Phosphorylation screening identifies translational initiation factor 4GII as an intracellular target of Ca(2+)/calmodulin-dependent protein kinase I. *J. Biol. Chem.* **278**:48570–48579.
 47. **Qin, X., and P. Sarnow.** 2004. Preferential translation of internal ribosome entry site containing mRNAs during the mitotic cell cycle in mammalian cells. *J. Biol. Chem.* **279**:13721–13728.
 48. **Raught, B., A. C. Gingras, S. P. Gygi, H. Imataka, S. Morino, A. Gradi, R. Aebersold, and N. Sonenberg.** 2000. Serum-stimulated, rapamycin-sensitive phosphorylation sites in the eukaryotic translation initiation factor 4GI. *EMBO J.* **19**:434–444.
 49. **Sui, G., C. Soohoo, E. B. Affar, F. Gay, Y. Shi, W. C. Forrester, and Y. Shi.** 2002. A DNA vector-based RNAi technology to suppress gene expression in mammalian cells. *Proc. Natl. Acad. Sci. USA* **99**:5515–5520.
 50. **Tomari, Y., and P. D. Zamore.** 2005. Perspective: machines for RNAi. *Genes Dev.* **19**:517–529.
 51. **Ventoso, I., R. Blanco, C. Perales, and L. Carrasco.** 2001. HIV-1 protease cleaves eukaryotic initiation factor 4G and inhibits cap-dependent translation. *Proc. Natl. Acad. Sci. USA* **98**:12966–12971.
 52. **Yan, R., W. Rychlik, D. Etchison, and R. E. Rhoads.** 1992. Amino acid sequence of the human protein synthesis initiation factor eIF-4 gamma. *J. Biol. Chem.* **267**:23226–23231.